Low-frequency scattering of Kelvin waves by continuous topography

By E. R. JOHNSON

Department of Mathematics, University College London, Gower Street,
London, WC1E 6BT, UK

This paper continues the analysis of Johnson (1990, hereinafter referred to as I) of the scattering of Kelvin waves by collections of ridges and valleys. General results, flow patterns and explicit solutions follow by restricting attention to waves whose period is long compared to the inertial period but without the additional further simplification introduced in I of approximating general features by stepped topography. A simple direct method is presented giving explicit formulae for the amplitude of the transmitted Kelvin wave and the scattered topographic long waves. A simple but accurate approximation to the solution is also given. The accuracy and usefulness of the apparently crude method of I are confirmed and a superior method presented for choosing the positions of steps in the approximation of general topography. Inviscid flows, the effects of weak dissipation and weak stratification, the form and relevance of the short-wave field over downslopes, the partition of mass and energy flux between the long-wave and short-wave fields and the size and form of higher-order effects are also discussed.

1. Introduction

The paper continues the discussion of low-frequency scattering of Kelvin waves presented in Johnson (1990, hereinafter referred to as I). A Kelvin wave travelling along the bounding wall of a rotating domain is incident upon a region of irregular bottom topography whose isobaths become parallel sufficiently far from the bounding wall and so support topographic Rossby waves. It is shown in I that in the low-frequency limit the flow field separates naturally into three regions: an outer-x region containing the incident and transmitted Kelvin waves; and outer-y region containing the scattered topographic long waves; and an inner, geostrophic region. The analysis in I is further simplified by approximating general profiles by stepped topography. This removes the difficulties caused by short waves over continuous topography and allows the flow pattern at the wall to be resolved using the analysis of wall–step junctions in Johnson (1985), Gill *et al.* (1986) and Johnson & Davey (1990). As the number of approximating steps increases, a narrow high-velocity layer forms where steps in downslopes meet the bounding wall. It is the purpose of the present paper to consider directly the case of continuous topography, quantifying the contribution of the short waves, analysing the structure of the wall layer, obtaining various general results, assessing the rate of convergence of the stepped approximation of I and presenting a superior method of choosing the positions of the jumps when approximating complex topography. A simple but accurate estimate for the amplitude of the transmitted Kelvin wave emerges as a corollary.

Section 2 introduces the equations of motion, discusses the separation of the flow

into distinct asymptotic regions and the matching between the regions, and presents explicit solutions and flow patterns for scattering by an upward escarpment. It is shown that the *amplitudes* of the transmitted and incident waves are equal for any similar topography not supporting short waves. Section 3 considers the flow field above downward escarpments, showing first that the *volume fluxes* of the incident and transmitted fields are equal and hence the amplitude of the transmitted Kelvin wave depends only on the fractional change of depth across the escarpment. A detailed solution and flow patterns are given for exponential topography and the form of the flow pattern for more general topography is discussed in sufficient detail for the subsequent analysis in §§4 and 5. Section 4 applies the methodology and results of §§2 and 3 to obtain the form of the long-wave field and the transmitted wave amplitude over a ridge of general profile and §5 gives analogous results for a general valley. Both sections include accurate approximations for the transmitted Kelvin wave amplitude that require only the form of the fundamental topographic long wave. Section 6 gives specific examples of this theory for an exponential ridge where the full solution can be found and for triangular ridges and valleys where explicit analytical forms are found for the relevant eigenfunctions. Section 7 extends the analysis and discusses some aspects in more detail. The filtering out of the short-wave field over non-exponential topography is shown to be equivalent to the effect of weak dissipation in barotropic flow where energy is destroyed in viscous wall layers, or weak stratification in inviscid flow where energy is transmitted as internal Kelvin waves confined close to the bounding wall. In both cases the long-wave field determined here is unaffected. Results are extended to non-planar bounding walls, locally non-rectilinear topography and topography with plateaux. The form and size of the higher-order (in frequency) terms giving the first corrections to the present solutions are noted. Appendix A considers the adjoint problem, showing that it differs from the usual form for non-rotating flow and obtaining the useful result that the *transmitted volume fluxes* of the original and adjoint problems are the same at all sub-inertial frequencies. Appendix B notes the extension of the present method to more irregular topography, showing that the stepped-topography analysis of I can be regarded as the simplest discretization of the continuous problem.

2. Governing equations and upward escarpments

Using the notation of I the equations governing a Kelvin wave of frequency ωf and unit amplitude incident on topography abutting the bounding wall of the semi-infinite domain $y \geqslant 0$ can be written

$$i\omega[\nabla \cdot (h\nabla\eta) - (1 - \omega^2)\,\eta] + \hat{z} \cdot (\nabla h \wedge \nabla\eta) = 0 \quad (y > 0), \tag{2.1}$$

$$i\omega\eta_y - \eta_x = 0 \quad (y = 0), \tag{2.2}$$

$$\eta \to e^{-y - i\omega x} \quad (x \to -\infty). \tag{2.3}$$

The surface elevation associated with the wave is $\mathrm{Re}\,\{\eta(x, y)\exp{(i\omega ft)}\}$; the local undisturbed depth is $h(x, y)$, scaled to unity for $-x \gg 1$; $\hat{z}$ is a unit vertical vector; and horizontal lengths have been scaled on the incident Rossby radius (figure 1a). It is noted in I that above stepped topography in the low-frequency limit ($\omega \ll 1$) there are three distinct regions: an outer-y region of long topographic waves where x and $Y = \omega y$ are fixed as $\omega \to 0$; an outer-x region containing the incident and transmitted Kelvin waves where $X = \omega x$ and y are fixed; and an inner, geostrophic region with
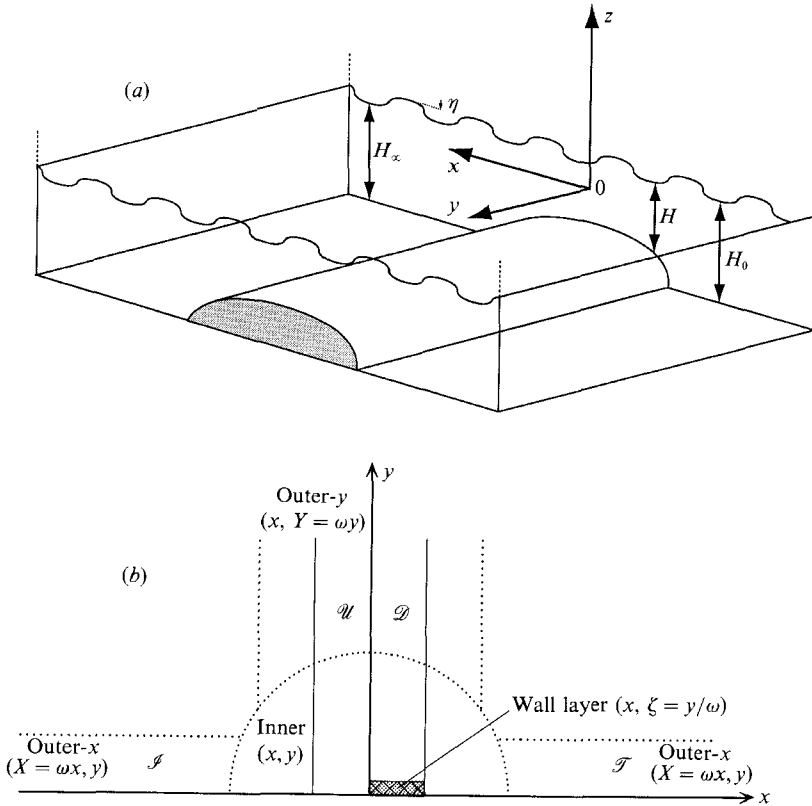
FIGURE 1. (a) The geometry considered. A Kelvin wave propagating along the wall $y = 0$ from a region of unit depth is incident upon a scattering region whose isobaths become parallel at large y. (b) The regions of flow and the relevant scales in the low-frequency limit. The incident, upslope, downslope and transmission regions are denoted $\mathscr{I}$, $\mathscr{U}$, $\mathscr{D}$, and $\mathscr{T}$.

x, y fixed as $\omega \to 0$. The possibility of X, Y fixed gives the quiescent ocean $\eta \equiv 0$ (figure 1b). Further, shorter lengthscales appear above continuous topography. These are confined to narrow layers in weakly dissipative flow (Johnson 1989a) and weakly stratified flow (Johnson 1991b) but occur everywhere above topography in purely inviscid barotropic flow (as in Johnson 1991a). They are discussed in greater detail in §3. For brevity of exposition the depth h is taken to be a function of x alone in §§2–6. Results for more complex bathymetry follow straightforwardly as in Johnson (1989b) and are noted in §7.

Consider an upward escarpment with constant unit depth ($h = 1$) in a region $\mathscr{I}$ ($x \leqslant W_- < 0$) containing the incident Kelvin wave, an upslope region $\mathscr{U}$ ($W_- \leqslant x \leqslant 0$) where the depth decreases ($h' < 0$), and a flat shallower ($h = h_\infty < 1$) region $\mathscr{T}$ ($x \geqslant 0$) containing the transmitted Kelvin wave. Downward escarpments are considered in §3. The analysis in Longuet-Higgins (1968) demonstrates that the upslope supports long waves carrying energy away from the wall and short waves carrying energy inwards. The sole source of energy in the present problem is the incident Kelvin wave and so causality precludes short waves above the upslope. The shortest scales in the upward escarpment problem are thus the escarpment width and the external Rossby radius.

2.1. *The inner, geostrophic region*

As noted in I the flow on the scale of the topography is geostrophic in the low-frequency limit with the surface elevation η acting as a streamfunction and the velocity vector given by $z \wedge \nabla \eta$. From (2.1) the inner geostrophic flow satisfies

$$\nabla h \wedge \nabla \eta = 0 \quad \text{if} \quad \nabla h \neq 0 \tag{2.4a}$$

$$h\nabla^2 \eta - \eta = 0 \quad \text{if} \quad \nabla h = 0, \tag{2.4b}$$

$$\eta_x = 0 \quad \text{on} \quad y = 0, \tag{2.5}$$

$$\eta \to e^{-y} \quad \text{as} \quad x \to -\infty. \tag{2.6}$$

Boundary condition (2.5) requires the surface elevation to be constant to leading order along the wall. Thus

$$\eta = 1 \quad (y = 0, \quad x = O(1)), \tag{2.7}$$

and the transmitted Kelvin wave has unit amplitude. More generally, *any geometry that does not support short outwardly propagating waves transmits Kelvin waves with undiminished amplitude in the low-frequency limit.*

Field equation (2.4a) shows that the surface elevation is constant along isobaths and flow follows isobaths. Combined with (2.7) this gives above the upslope

$$\eta \equiv 1 \quad \text{on} \quad \mathscr{U}, \quad (y = O(1)). \tag{2.8}$$

The inner flow is stagnant to leading order and the surface is flat. If only the amplitude of the transmitted wave is of interest the problem for upward escarpments is complete. However, the analysis for the more involved problems of scattering by ridges and valleys can be shortened by establishing a general framework for solutions by solving for the complete flow field over the escarpment. The solution splits naturally into the incident and transmitted Kelvin waves, the outer long-wave field over the upslope $\eta_0(x, Y)$, and an inner geostrophic flow $\eta_1(x, y)$ matching the two wavefields in the neighbourhood of the origin.

2.2. *The long waves*

From (2.1) the wavefield η_0 varying on the long-y scale satisfies

$$\partial_x(h\partial_x \eta_0) - \eta_0 - ih' \partial_Y \eta_0 = 0, \tag{2.9}$$

and has separated solutions of the form

$$\eta_0(x, Y) = \phi(x)\,e^{-i\lambda Y}, \tag{2.10}$$

provided

$$h\phi'' + h'\phi' - \phi - \lambda h'\phi = 0. \tag{2.11}$$

Away from the upslope h' vanishes and so

$$\phi = \begin{cases} c_1 \exp(x) & \text{in} \quad \mathscr{I}, \\ c_2 \exp(-h_\infty^{-\frac{1}{2}} x) & \text{in} \quad \mathscr{T}, \end{cases} \tag{2.12}$$

for some constants c_1 and c_2. Thus (2.11) is to be solved over the upslope $\mathscr{U}$ subject to the boundary conditions

$$\phi' - \phi = 0, \quad x = W_-, \tag{2.13a}$$

$$\phi' + h_\infty^{-\frac{1}{2}}\phi = 0, \quad x = 0, \tag{2.13b}$$

guaranteeing continuity of ϕ and ϕ' across $x = W_-, 0$. Since h' is single-signed (2.11)

and (2.13) form a standard Sturm–Liouville problem with positive eigenvalues $0 < \lambda_1 < \lambda_2 < \dots$ and sole accumulation point infinity. The corresponding eigenfunctions $\phi_1, \phi_2, \dots$ have none, one, ... zero-crossings, with zeros of successive modes interlacing, and form a complete set with orthogonality relation

$$\int_{\mathcal{U}} h' \phi_n \phi_m \, \mathrm{d}x = 0 \quad n \neq m. \tag{2.14}$$

The scattered long-wave field above the upslope can thus be expanded as

$$\eta_0(x, Y) = \sum_{n=1}^{\infty} \alpha_n \phi_n(x) \, \mathrm{e}^{-\mathrm{i}\lambda_n Y}, \tag{2.15}$$

where the unknown modal amplitudes α_n remain to be determined.

2.3. *Matching the inner- and outer-y solutions*

Denote the inner limit of the outer-y long-wave solutions by $g(x)$. Then

$$g(x) \equiv \lim_{Y \to 0} \eta_0(x, Y) = \eta_0(x, 0) = \sum_{n=1}^{\infty} \alpha_n \phi_n(x). \tag{2.16}$$

This matches the outer limit of the inner geostrophic flow, i.e.

$$g(x) = \lim_{y \to \infty} \eta(x, y) = 1 \quad \text{on} \quad \mathcal{U}, \tag{2.17}$$

from (2.7), uniquely determining the amplitudes α_n as

$$\alpha_n = \int_{\mathcal{U}} (-h') \phi_n \, \mathrm{d}x \Big/ \int_{\mathcal{U}} (-h') \phi_n^2 \, \mathrm{d}x. \tag{2.18}$$

The numerator is the inward mass flux associated with eigenfunction n and the denominator its energy flux.

The total mass flux carried by the long waves is

$$\int_{-\infty}^{\infty} \frac{\partial \eta_0}{\partial x}(x, 0) h \, \mathrm{d}x = \int_{-\infty}^{\infty} g' h \, \mathrm{d}x = \int_{\mathscr{I}} g' \, \mathrm{d}x + h_\infty \int_{\mathscr{T}} g' \, \mathrm{d}x = g(W_-) - h_\infty g(0) = 1 - h_\infty. \tag{2.19}$$

As the mass flux of the transmitted Kelvin waves is h_∞, mass is conserved. Similarly the energy flux of the long waves, normalized on the energy flux of the incident Kelvin wave, is

$$2 \int_{-\infty}^{\infty} \eta_0 \frac{\partial \eta_0}{\partial x}(x, 0) h \, \mathrm{d}x = 2 \int_{-\infty}^{\infty} g g' h \, \mathrm{d}x = 2 \int_{\mathscr{I}} g g' \, \mathrm{d}x + 2 h_\infty \int_{\mathscr{T}} g g' \, \mathrm{d}x$$
$$= g^2(W_-) - h_\infty g^2(0) = 1 - h_\infty. \tag{2.20}$$

As the normalized energy flux of the transmitted Kelvin wave is h_∞, energy is also conserved. Note that g given by (2.17) does not satisfy (2.13) and so expansion (2.16) although absolutely convergent exhibits Gibbs phenomena at $x = W_-, 0$ caused by

the discontinuity in bottom slope there. The slope discontinuity does not modify the zero-order flow but drives a high-x-wavenumber component to the flow of order $\omega^{\frac{1}{2}}$. These higher-order effects are discussed briefly in §7.

2.4. *The geostrophic flow over the flat bottom*

Above the escarpment the leading-order flow field is given completely by (2.15) with the α_n determined by (2.18). The remainder of the leading-order flow field is determined by the inner geostrophic solution over the flat incident and transmission regions away from the escarpment.

Consider first the incident region $\mathscr{I}$. The solution here can be written

$$\eta = e^{-y-iX} + \eta_0(x, Y) + \eta_i(x, y), \tag{2.21}$$

where the geostrophic term η_i satisfies (2.4b) with $h = 1$. The boundary conditions on η_i come from the specified surface elevation at the wall, matching the surface elevation across $x = W_-$, and requiring the solution to be bounded at large distance. These give

$$\eta_i = -e^{-y} \quad (x = W_-, \quad y > 0), \tag{2.22}$$

$$\eta_i = -g(x) = -\exp(x - W_-) \quad (y = 0, \quad x < W_-), \tag{2.23}$$

$$\nabla \eta_i \to 0 \quad (x \to -\infty, \quad y \to \infty). \tag{2.24}$$

The solution of (2.4b) subject to (2.22)–(2.24) follows as in I as

$$\eta_i = \frac{2}{\pi} \int_0^\infty [(1/l - l/\kappa^2) \exp(-\kappa |x - W_-|) - \exp(-|x - W_-|l)] \sin ly \, dl, \tag{2.25}$$

where $\kappa = (l^2 - 1)^{\frac{1}{2}}$.

In the transmission region $\mathscr{T}$ the surface elevation can be written as

$$\eta = \exp[-h_\infty^{-\frac{1}{2}}(y + iX)] + \eta_0(x, Y) + \eta_i(x, y), \tag{2.26}$$

with η_i given by (2.25) with, however, $W_- = 0$ and $\kappa = (l^2 + h_\infty^{-1})^{\frac{1}{2}}$.

The expansions of this section have been derived assuming that h' is strictly negative in $\mathscr{U}$. It is noted in §7 that the results here are unaltered for profiles with flat regions, i.e. for the wider class of escarpments where $h' \leqslant 0$.

2.5. *A uniformly sloping escarpment*
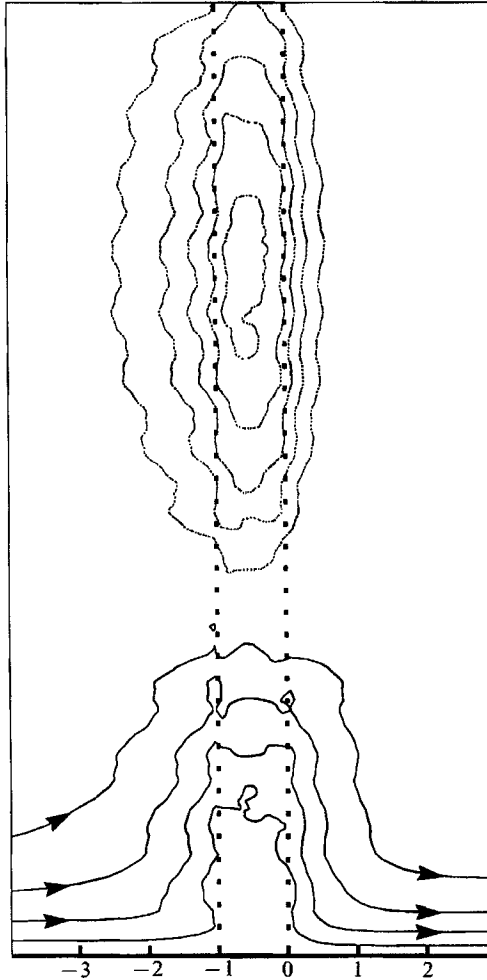
Consider the continuous linear upward escarpment given by

$$h = \begin{cases} 1, & x \leqslant -W, \\ 1 + (h_1 - 1)(x/W + 1), & -W \leqslant x \leqslant 0, \\ h_1, & x \geqslant 0. \end{cases} \tag{2.27}$$

For $-W \leqslant x \leqslant 0$ introduce $X = [X_0^2 + \text{sgn}(1 - h_1)|x|]^{\frac{1}{2}}$ so

$$h = (X/X_1)^2 \quad (X_0 \leqslant X \leqslant X_1), \tag{2.28}$$

where $X_0^2 = Wh_1/|1 - h_1|$ and $X_1^2 = W/|1 - h_1|$. Then the long-wave equation (2.11) becomes

$$X^2 \phi_{XX} + X \phi_X - 4X^2(\lambda - X_1^2) \phi = 0 \quad (X_0 \leqslant X \leqslant X_1), \tag{2.29}$$

Figure 2. Contours of surface elevation for a Kelvin wave of unit amplitude incident on an escarpment rising linearly from unit depth in the incident region $x \leqslant -1$ to depth $h_1 = 0.5$ in the transmission region. The contour interval here and in later figures is 0.2 with positive contours continuous, negative contours finely dotted, the zero contour omitted for clarity and the changes of slope at $x = -W$, 0 dashed. The surface is plotted at time $t = 0$ when the incident wave has maximum instantaneous amplitude at $x = 0$. Since only long waves are present in this example the contours are streamlines of the flow to leading order in the frequency ω. Here $\omega = 0.1$.

Bessel's equation of order zero. The solution of (2.29) subject to (2.13a) is

$$\phi = (Y^1/J^0) J_0(kX) - (J^1/J^0) Y_0(kX) \quad (-W \leqslant x \leqslant 0), \tag{2.30}$$

$$
\left.
\begin{aligned}
Y^1 &= 2X_1 Y_0(kX_1) - kY_1(kX_1), \\
J^1 &= 2X_1 J_0(kX_1) - kJ_1(kX_1), \\
J^0 &= Y^1 J_0(kX_0) - J^1 Y_0(kX_0),
\end{aligned}
\right\} \tag{2.31}
$$

where J_0, J_1, Y_0, Y_1 are the Bessel functions of the first and second kind and $k^2 = 4(\lambda - X_1^2)$ so

$$\lambda = \tfrac{1}{4}k^2 + X_1^2 > 0. \tag{2.32}$$

Substituting (2.30) into (2.13b) gives the eigenfunction relation determining k and the λ_n as

$$kh_1^{\frac{1}{2}} [Y^1 J_1(kX_0) - J^1 Y_1(kX_0)] + 2X_0 J^0 = 0. \tag{2.33}$$
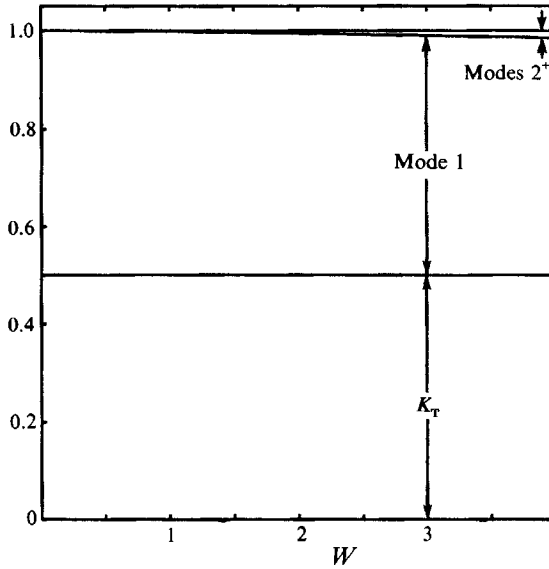
FIGURE 3. The distribution of energy flux in the scattered field above an upward linear escarpment as a function of the escarpment width W for depth $h_1 = 0.5$. The fluxes have been normalized on the flux of the incident wave with the contributions of the long topographic waves denoted 1, 2^+ and that of the transmitted Kelvin wave, K_T. It is shown in the text that the transmitted Kelvin wave always carries the fraction h_1 of the incident flux. As short waves are precluded by the radiation condition, energy is conserved within the long-wave field. The scattered field is dominated by the fundamental mode – the sole surviving mode for $W \ll 1$ as in the vertical escarpment of I.

Each of (2.30)–(2.33) is even in k and thus it is sufficient to take $k > 0$. Once the λ_n and k have been found the amplitudes α_n of the scattered long-wave modes follow from (2.18). The integral in the numerator can be obtained explicitly by noting that h' is constant for $x \neq -W, 0$ and so the long-wave equation (2.11) with conditions (2.13) gives

$$\int_{\mathscr{U}} (-h')\,\phi_n\,\mathrm{d}x = (-h')\,(1+\lambda_n\,h')^{-1} \int_{\mathscr{U}} (h\phi_n')'\,\mathrm{d}x$$

$$= [h_1^{\frac{1}{2}}\,\phi_n(0) + \phi_n(-W)]\,h'/(1+\lambda_n\,h'). \quad (2.34)$$

Figure 2 gives the surface elevation derived from (2.15), (2.18), (2.25) and (2.26) for an escarpment of width $W = 1$ rising to depth $h_1 = 0.5$. As the surface elevation of the incident wave rises and falls through a cycle a topographic wave pulse, consisting mainly of the fundamental mode, is generated and propagates outwards along the escarpment.

The partition of energy amongst the scattered modes also shows the importance of the fundamental mode. The energy flux carried by mode n in expansion (2.15) is

$$\alpha_n^2 \int (-h')\,\phi_n^2 = \left[\int (-h')\,\phi_n\,\mathrm{d}x \right]^2 / \int (-h')\,\phi_n^2. \quad (2.35)$$

Figure 3 gives the distribution of energy flux among the transmitted Kelvin wave and the long waves as a function of the escarpment width for $h_1 = 0.5$. The long-wave energy is carried almost entirely by the fundamental mode. As $W \to 0$ the escarpment steepens and the wavelengths of all modes but the fundamental vanish as do their

amplitudes in the scattered field. The wavelength of the fundamental mode approaches $(1 - h_1^{\frac{1}{2}})^{-1}$, the value for a vertical step. This is unity (the reciprocal of the external Kelvin wave speed) for very shallow transmission regions ($h_1 \ll 1$) and increases monotonically without bound as the escarpment height decreases and h_1 approaches unity.† The amplitude of the scattered fundamental mode remains non-zero as $W \to 0$, with the mode carrying the whole fraction $1 - h_1$ of the incident energy scattered away from the wall, as in I. This dominance of the fundamental mode forms the basis for accurate approximations of the more complex fields over ridges and valleys in §§4 and 5.

3. Downward escarpments

Consider a downward escarpment with constant unit depth ($h = 1$) in the incident region $\mathscr{I}$ ($x \leqslant 0$), a downslope region $\mathscr{D}$ ($0 \leqslant x \leqslant W_+$) where h' is positive and the depth increases, and a flat deeper ($h = h_\infty > 1$) transmission region $\mathscr{T}$ ($x \geqslant W_+$). This escarpment supports long waves carrying energy towards the wall and short waves carrying energy outwards. Causality thus precludes long waves above the downslope but allows short scattered waves with inwardly propagating phase but outward group velocity. The short waves have scales $\omega \ll 1$ in their direction of propagation and unity along wave fronts. For general escarpments the ray paths of short waves are not straight (Smith 1972) and so in the rectilinear coordinates (x, y) the wavefield has scale ω in both x and y. These short scales are responsible for the formidable difficulties in obtaining both numerical (Killworth 1989) and complete explicit analytical solutions at low frequencies. The analysis in Johnson (1991a) extends directly to show that although the short waves carry energy outwards they carry no net instantaneous mass flux. *The mass flux in the Kelvin wave field is conserved over escarpments that do not support outwardly propagating long waves.* Independently of the escarpment profile the transmitted Kelvin wave carries unit mass and so has reduced amplitude $h_\infty^{-1} < 1$. The transmitted wave carries energy flux h_∞^{-1} and so a flux $1 - h_\infty^{-1}$ is scattered into the short waves to be carried away from the wall. If only the amplitude of the transmitted wave is of interest the problem for downward escarpments is complete. However, as for upward escarpments in §2, examination of the complete flow field establishes a framework for discussing scattering by more general topography.

3.1. *The wavefield above an exponential downslope*

Above exponential topography ray paths are straight, solutions simplify, and the complete scattered field can be obtained analytically. Consider the continuous escarpment

$$h = \begin{cases} 1, & x \leqslant 0, \\ e^{\beta x}, & 0 \leqslant x \leqslant W_+, \\ h_\infty, & x \geqslant W_+, \end{cases} \tag{3.1}$$

where $\beta = (1/W_+) \log h_\infty$ ($\beta > 0$ for $h_\infty > 1$), and separate the phase and group velocity components by writing (see Johnson 1991a)

$$\eta(x, y) = \exp(\mathrm{i}\beta y/\omega)\, \Psi(x, Y) \quad \text{over } \mathscr{D}. \tag{3.2}$$

† For $h_1 > 1$, downward escarpments, the fundamental wavelength decreases from infinity as h_1 increases and, as $h_1 \to \infty$, approaches once again the reciprocal of the external Kelvin wave speed for the deeper side.

Restoring time-dependence shows that the factor $\exp{(\mathrm{i}\omega t + \mathrm{i}\beta y/\omega)}$ gives the rapidly varying incoming phase of the short waves. The slowly varying envelope $\Psi(x, Y)$ satisfies

$$\Psi_{xx} + \beta\Psi_x - h^{-1}\Psi + \mathrm{i}\beta\Psi_Y = 0 \quad \text{over } \mathscr{D}. \tag{3.3}$$

The boundary conditions on envelope are discussed in detail in Johnson (1991 a) and require that to leading order no flow crosses escarpment edges:

$$\Psi = 0 \quad (x = 0, W_+, \quad y > 0), \tag{3.4}$$

Substituting form (3.2) into the impermeability condition (2.2) gives at the wall

$$\Psi_x + \beta\Psi = (h\Psi)_x = 0 \quad \text{over } \mathscr{D} \quad (y = 0). \tag{3.5}$$

Integrating this boundary condition across the escarpment gives $h\Psi = 1$, i.e. the surface elevation at the wall is

$$\eta = h^{-1} \quad \text{over } \mathscr{D} \quad (y = 0). \tag{3.6}$$

It is shown below that (3.6) holds for all downward escarpments.

Equation (3.3) has wavelike solutions of the form

$$\Psi(x, Y) = \psi_n(x)\,\mathrm{e}^{-\mathrm{i}\mu Y}, \tag{3.7}$$

provided the μ_n, ψ_n satisfy

$$h\psi'' + h'\psi' - \psi + \mu h'\psi = 0. \tag{3.8}$$

Equation (3.8) is the long-wave equation of §2 with the direction of propagation reversed, giving, however, outwardly propagating energy again here as the sign of the slope is also reversed. The eigensolutions μ_n, ψ_n, satisfying the no-flux conditions (3.4) at the escarpment edges, have the same general properties as the λ_n, ϕ_n and so the wavefield satisfying the wall condition (3.6) can be expanded as

$$\Psi(x, Y) = \sum_{n=1}^{\infty} \alpha_n \psi_n(x)\,\mathrm{e}^{-\mathrm{i}\mu_n Y}, \tag{3.9}$$

where

$$\alpha_n = \int_{\mathscr{D}} (h'/h)\,\psi_n \,\mathrm{d}x \Big/ \int_{\mathscr{D}} h'\psi_n^2 \,\mathrm{d}x. \tag{3.10}$$

An analogous evaluation to (2.19) shows that the total outward short-wave energy flux is $1 - 1/h_\infty$ as required by energy conservation. Mass is conserved as a matter of course since the amplitude of the transmitted Kelvin wave is determined by requiring the short waves to carry no mass.

3.2. *The geostrophic component over the flat bottom*

The remainder of the leading-order flow field consists of an inner geostrophic solution $\eta_i(x, y)$ over $\mathscr{I}$ and $\mathscr{T}$. Since the short waves carry no mass this flow decouples entirely from the flow above the downslope and is thus the same for all escarpments. There is a sink/source pair of strength unity (strictly, of strength $\cos\omega t$ once time-dependence is restored) where the escarpment edge meets the wall at $(x, y) = (0, 0)$ of precisely the form discussed in detail in Johnson (1985) for a vertical escarpment meeting a bounding wall and a similar source/sink pair (also with mass flux, $h\eta$, unity) at the other edge–wall junction $(W_+, 0)$. Consider first the incident region $\mathscr{I}$. The solution here can be written

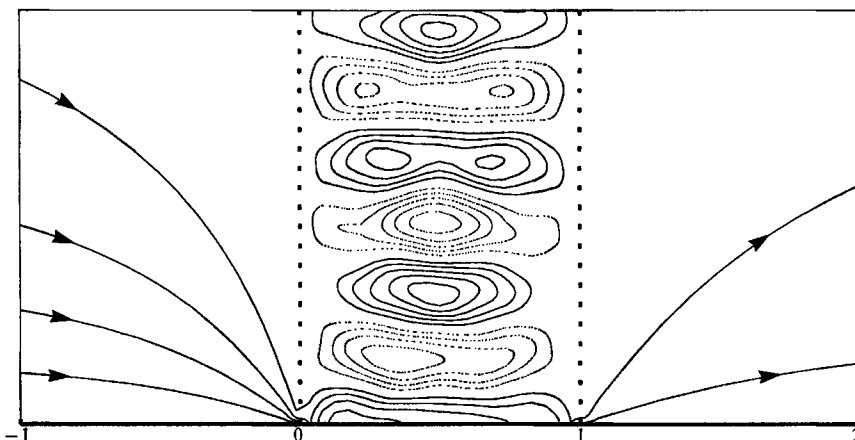$$\eta = \mathrm{e}^{-y-\mathrm{i}X} + \eta_1(x, y), \tag{3.11}$$

FIGURE 4. Contours of surface elevation for a Kelvin wave incident on a downward escarpment of width $W = 1$ where the depth increases exponentially from unity to $h_1 = 2$. Away from the slope the contours are streamlines for the flow but the short scales above the slope contribute additional terms to the velocity components. The phase above the slope propagates towards the wall but the energy of the waves is scattered outwards.

where the geostrophic term η_1 satisfies the same field equation (2.4*b*) and boundary conditions (2.22), (2.24) as η_1 in §2.4 with, however, the wall condition (2.23) replaced by

$$\eta_1 = 0 \quad (y = 0, x < 0). \tag{3.12}$$

An expression for η_1 of form (2.25) follows directly as in §2.4 as does the analogous expression to (2.26) for η and η_1 in the transmission region $\mathscr{T}$.

The inclusion of the geostrophic flow completes the analytical description of the surface elevation. However, unlike the eigensolutions for the linearly sloping escarpment of §2, the solutions μ_n, ψ_n for exponential slopes have no useful simple analytical form in free-surface flows (although simple expressions exist in the rigid-lid limit, $W_+ \to 0$). Numerical results follow most straightforwardly by solving (3.9) directly. Routine D02KEF of the Numerical Algorithms Group library using a Pruefer substitution proved accurate and highly efficient, extending directly to the more complex topographies of §6. Once the eigenfunctions are found, (3.10) gives the modal amplitudes directly and fast Fourier inversion gives the geostrophic component η_j. Figure 4 gives contours of surface elevation for an escarpment of width $W_+ = 1$ and transmission region depth $h_\infty = 2$. Over each cycle of the incident Kelvin wave one cycle of the short topographic wave arrives and is absorbed at the wall. Away from the slope the contours are streamlines and in particular the wall coincides with the streamline $\eta = 1$ in $x \leqslant 0$ and $\eta = 1/h_\infty$ in $x \geqslant W$. Above the slope additional terms contribute to the velocity components so contours of η are no longer streamlines and intersect the wall although the normal velocity vanishes there. The source/sink pairs at $(0, 0)$ and $(W_+, 0)$ are clearly visible.

3.3. *General downslopes*

The wavefield above non-exponential downslopes does not decompose straight-forwardly into modes and hence an explicit solution is not direct. However, the behaviour above the slope but close to the wall can be described in detail. This is sufficient to determine the amount of energy scattered into short waves even though

the subsequent wave paths cannot be determined explicitly. When even vanishingly small dissipation is included this layer gives the whole flow above the downslope and the energy scattered into short waves is destroyed there.

For arbitrary $h(x)$ consider a region against the wall of thickness of order the wavelength of the short waves. Introduce $\zeta = y/\omega$ so the field equation (2.1) and the impermeability condition (2.2) become

$$ih\eta_{\zeta\zeta} + h'\eta_\zeta = 0, \qquad (3.13)$$

$$i\eta_\zeta - \eta_x = 0 \quad (\zeta = 0). \qquad (3.14)$$

The general solution of (3.13) can be written

$$\eta = b(x) + [a(x) - b(x)]\exp{(ih'\zeta/h)} \quad \text{over } \mathscr{D} \quad (y = O(\omega)), \qquad (3.15)$$

where $a(x)$ and $b(x)$ are arbitrary functions with $a(x)$ giving the surface elevation at the wall ($\zeta = 0$) so

$$a(0) = 1, \quad a(W_+) = A, \qquad (3.16)$$

for incident amplitude unity and transmitted amplitude A. The first term in (3.15) is the contribution in the region from external long waves or geostrophic flow and so does not vary with y on this short scale. The second term gives the amplitude $a(x) - b(x)$ of the short waves with rapidly varying inwardly propagating (since $h' < 0$) phase. Substituting (3.15) into (3.14) gives

$$(ha)' = h'b \quad \text{over } \mathscr{D} \quad (\zeta = 0). \qquad (3.17)$$

Since long waves are precluded above downward escarpments $b(x)$ is identically zero in the present case and (3.17) integrates immediately along the wall to extend (3.6) to arbitrary downslopes. Within this region

$$\eta = h^{-1}\exp{[(ih'/h)\,\zeta]}. \qquad (3.18)$$

For downward escarpments ($h' > 0$) (3.18) consists of short waves with inwardly propagating phase carrying energy outwards.

The analysis in Johnson (1989a) extends to show that the inclusion of even vanishingly small viscosity introduces an order-unity negative part to the coefficient of ζ in (3.18) and hence causes short-wave energy to be dissipated within a wall-layer of thickness ω. This layer carries all the Kelvin wave mass flux but dissipates a fraction $1 - h_\infty^{-1}$ of the incident energy. Outside the layer the flow field becomes simply

$$\eta \equiv 0 \quad \text{over } \mathscr{D} \quad (y > 0), \qquad (3.19)$$

and the scattered short-wave field is absent. Similarly, the analysis of inviscid scattering of coastally trapped waves in Johnson (1991b) shows the barotropic flow on the geostrophic and long-wave scales to be unaffected by weak stratification, i.e. when $B \ll 1$ where the stratification parameter $B = N_0 H/fL$ for buoyancy frequency N_0, depth H and escarpment width L. Moreover, if $\omega \ll B \ll 1$ the barotropic short waves are absent and the energy scattered out of the barotropic long-wave field is scattered into a set of transmitted internal Kelvin waves to be carried towards $x = \infty$ confined closely to the wall $y = 0$ in a thin layer of thickness $B \ll 1$. For a downward escarpment the transmitted external Kelvin wave carries the whole incident mass flux and a fraction h_∞^{-1} of the incident energy flux, and the internal Kelvin wave field carries no mass but transmits the remaining fraction $1 - h_\infty^{-1}$ of the incident energy flux.

Since the short-wave components of the wave field for inviscid barotropic flow above general topography have no simple analytical expression the analysis for general topography in the remainder of this paper concentrates on determining completely the barotropic long-wave and geostrophic components of the flow and the short-wave component only within a distance ω of the wall. The above results show however that fields omitting short waves give the leading-order flow patterns outside thin wall layers for weakly dissipative barotropic flow and for weakly stratified flows where $\omega \ll B \ll 1$. The full flow patterns including short waves can of course be given for piecewise exponential topography.

4. Ridges

A flat-topped ridge can be formed from an upward escarpment followed by a downward escarpment. If the two escarpments are separated by two or more Rossby radii the analysis of §§2 and 3 can be applied independently giving outwardly propagating long waves over the upslope and an outwardly propagating envelope of short waves (with inwardly propagating phase) over the downslope. As in I, the amplitude of the transmitted wave is given by $H_1/H_\infty < 1$, the ratio of the minimum depth over the ridge to the depth after the ridge. For narrower ridges the two wavefields interact.

4.1. *The long waves and the outer-y region*

Consider a continuous ridge with unit depth ($h = 1$) in an incident region $\mathscr{I}$ ($x \leqslant W_-$), monotonic decreasing depth ($h' < 0$) in an upslope region $\mathscr{U}$ ($W_- < x < 0$), monotonic increasing depth in a downslope region $\mathscr{D}$ ($0 < x < W_+$), and a flat ($h = h_\infty$) transmission region $\mathscr{T}$ ($W_+ \leqslant x$). Ridges with plateaux are discussed in §7 and more general profiles in Appendix B. In weakly dissipative flow short waves are confined to wall layers and so above the ridge the leading-order surface elevation varies only on the long-wave scale $Y = \omega y$. This long-wave field $\eta_0(x, Y)$ satisfies (2.9) and can be decomposed into wave modes of form (2.10) satisfying (2.11) and boundary conditions (2.13) at the edges of the ridge. As h' is not single-signed the eigenvalue problem for the wave modes is no longer of standard Sturm–Liouville form. However similar arguments apply and the oscillation theorem (Ince 1927, chap. 10) implies that problem (2.11), (2.13) has countably many distinct real eigenvalues with two accumulation points at $\pm \infty$. The eigenvalues can be labelled

$$\ldots < \lambda_{-n} < \ldots < \lambda_{-2} < \lambda_{-1} < 0 < \lambda_1 < \lambda_2 < \ldots < \lambda_n < \ldots . \tag{4.1}$$

To each eigenvalue there corresponds exactly one eigenfunction. The eigenfunctions divide into two groups. Those corresponding to positive eigenvalues (outwardly propagating long-waves) are oscillatory above upslopes and decay exponentially above downslopes and those for negative eigenvalues (inwardly propagating long waves) are oscillatory above downslopes and decay above upslopes. Within each group the zeros of consecutive eigenfunctions interlace. Multiplying (2.11) by ϕ and integrating from $-\infty$ to ∞ gives a variational principle of the same form as in Johnson (1989d) for the λ_n, ϕ_n,

$$\lambda^{-1} = -\int_{-\infty}^{\infty} h'\phi^2 \, dx \bigg/ \int_{-\infty}^{\infty} [h(\phi')^2 + \phi^2] \, dx. \tag{4.2}$$

For an eigenfunction the numerator gives the associated energy flux and the

denominator the energy density, the first term giving the kinetic energy and the second the potential energy. The variational principle furnishes the inner product and energy norm

$$\langle f_1, f_2 \rangle = \int_{-\infty}^{\infty} (h f_1' f_2' + f_1 f_2) \, \mathrm{d}x, \quad \| f \|^2 = \langle f, f \rangle. \tag{4.3}$$

The eigenfunctions form an orthogonal set and any function orthogonal to each ϕ_n corresponds to $\lambda^{-1} = 0$ in (4.2) and hence vanishes above non-flat regions of finite width. The ϕ_n thus form a complete set for topographies without plateaux. Let $g(x)$ be the inner limit of the outer long-wave solution as in §2. Then g has the unique expansion

$$g(x) = \sum_{n=-\infty}^{\infty} \alpha_n \phi_n(x), \quad \alpha_n = \langle g, \phi_n \rangle / \| \phi_n \|^2. \tag{4.4}$$

Note that $\int_{-\infty}^{\infty} h' f_1 f_2 \, \mathrm{d}x$ no longer yields a positive definite inner product for non-monotonic h as $\int_{-\infty}^{\infty} h' \phi_n^2 \, \mathrm{d}x$ is positive for $n < 0$ and negative for $n > 0$. It does however yield the simpler alternative expression for the α_n,

$$\alpha_n = \int_{-\infty}^{\infty} h' g \phi_n \, \mathrm{d}x \bigg/ \int_{-\infty}^{\infty} h' \phi_n^2 \, \mathrm{d}x, \tag{4.5}$$

where the denominator is non-zero by (4.2). The radiation condition, that the incident Kelvin wave is the sole energy source, precludes incoming waves and so constrains g to be orthogonal to the ϕ_n for $n < 0$, i.e.

$$\alpha_n = 0, \quad \int_{-\infty}^{\infty} h' g \phi_n \, \mathrm{d}x = 0, \quad n = -1, -2, \dots, \tag{4.6}$$

giving an outer solution of precisely the form (2.15), (2.16) of §2.

4.2. *The wall layer*

Above the ridge on the inner scales x, y the flow follows bathymetry by (2.4 a). The outer limit ($y \to \infty$) of this inner geostrophic flow matches $g(x)$, the inner limit of the long-wave solution. Thus for the present case with h a function of y alone and in the weakly dissipative limit

$$\eta = g(x) \quad \text{over } \mathscr{U}, \mathscr{D} \quad (y = O(1)). \tag{4.7}$$

Equation (4.7) forms the outer boundary condition for the long-wave part of the wall-layer solution (3.15). Thus the flow in the wall layer is given by (3.15) with $b(x) \equiv g(x)$, where the first term in (3.15) is the long-wave contribution and the second term the short waves within the layer. Above $\mathscr{D}$ the slope h' is positive and this second term gives inward phase and outward energy in inviscid flow or exponentially decaying waves in weakly dissipative flow. Boundary condition (3.17) becomes

$$(ha)' = h'g, \quad \text{over } \mathscr{D} \quad (\zeta = 0), \tag{4.8}$$

which can be rewritten

$$-hv = [(a - g) h]', \tag{4.9}$$

where $-v = -g'(x)$ is the inward velocity in the geostrophic region. Equation (4.8) thus expresses conservation of mass, stating that the mass flux coming into the layer is equal to the rate of increase of mass carried by the layer.

Above the upslope $\mathscr{U}$ the slope h' is negative and the second term in (3.15) would represent short waves with outward phase and so inward energy (precluded by causality) in inviscid flow or disturbances growing exponentially with distance from the wall in weakly dissipative flow. Hence this term vanishes giving the simple solution

$$\eta = a(x) = g(x) \quad \text{over } \mathscr{U} \quad (y = O(\omega)). \tag{4.10}$$

There is no wall-layer above upslopes and the geostrophic flow (4.7) extends to the wall. The impermeability condition (2.2) thus requires

$$\eta_x = a'(x) = g'(x) = 0 \quad \text{over } \mathscr{U}. \tag{4.11}$$

The free surface is level above upslopes and the flow is stagnant to leading order.

The constraints on $a(x)$ and $g(x)$ implied by (4.8) and (4.11) holds for any combination of upslopes and downslopes. Continuity of surface elevation along the wall requires $a(W_-)$ to be unity and so for a simple ridge (4.11) integrates to become

$$a(x) \equiv 1, \quad g(x) \equiv 1 \quad \text{over } \mathscr{U}. \tag{4.12}$$

Combining this with (4.8) gives the surface elevation at the wall $a(x)$ in terms of the inner limit $g(x)$ of the long-wave field,

$$a(x) = \begin{cases} 1, & \text{over } \mathscr{I} \text{ and } \mathscr{U}, \\ [h(x_0) + \int_0^x h'g\,\mathrm{d}x]/h(x), & \text{over } \mathscr{D}, \\ A, & \text{in } \mathscr{T}, \end{cases} \tag{4.13}$$

so the transmitted amplitude A is given by

$$A = \left[h(0) + \int_{\mathscr{D}} h'g\,\mathrm{d}x\right]\bigg/h(W) = \left[h(0) + \sum_{n=1}^{\infty} \alpha_n \int_{\mathscr{D}} h'\phi_n\,\mathrm{d}x\right]\bigg/h(W) \tag{4.14}$$

from (2.16) where the amplitudes α_n of the long-wave modes have yet to be determined.

4.3. *Geostrophic flow over the flat bottom*

Once the α_n are known the surface elevation over the ridge is given by (2.15) and the Kelvin wave amplitude A by (4.14). The remainder of the flow field consists of the inner geostrophic solutions $\eta_i(x,y)$ in the incident and transmitted regions. In the incident region $\mathscr{I}$ the surface elevation is precisely (2.21) with η_i given by (2.25): all the incident mass flux turns to travel outwards along the upslope.

The flow in the transmission region is more complex with the mass flux of the transmitted Kelvin wave being supplied over two different paths. The surface elevation at the ridge edge $x = W_+$ in the geostrophic region outside the wall layer is $\mathscr{L} = g(W_+)$ and hence corresponds to a mass flux $h_\infty\mathscr{L}$ carried inwards over the flat bottom beside the ridge edge by the long-wave field. This flux turns in the neighbourhood of the origin to join a flux $h_\infty[a(W_+) - g(W_+)] = h_\infty(A - \mathscr{L})$ that is entrained into the wall layer above the downslope and carried in the layer to spread over the flat bottom from a source at $(x,y) = (W_+, 0)$. Together these fluxes give the transmitted flux $h_\infty A$. The flow in region $\mathscr{T}$ is thus of form (2.26) where η_i satisfies (2.4b) with $h = h_\infty$ and boundary conditions

$$\eta = -A \exp(-y) \quad (x = W_+, y > 0), \tag{4.15a}$$

$$\eta = -\mathscr{L} \exp(W_+ - x) \quad (x > W_+, y = 0). \tag{4.15b}$$

An expression of form (2.25) for η_i follows straightforwardly. Section 6 discusses flow patterns derived from these expressions for ridges with exponential and triangular profiles.

4.4. Matching the inner- and outer-y regions

It remains to determine the α_n. For a simple ridge it is most direct first to determine the amplitude of the long waves that superpose to satisfy (4.12) over $\mathcal{U}$ and then to evaluate $a(x)$ by substituting (2.16) for $g(x)$ over $\mathcal{D}$ in (4.12). Methods for more complex topography are discussed in Appendix B. Although the long-wave field over $\mathcal{U}$ could be obtained by collocation a more robust and transparent method is given by least-squares fitting with weighting function $-h'$ (which remains positive over $\mathcal{U}$). Define the squared deviation from (4.12) of g given by (2.16) by

$$D = \int_{\mathcal{U}} (g-1)^2(-h')\,\mathrm{d}x, \tag{4.16}$$

and choose the α_n to minimize D. At a minimum $\partial D/\partial \alpha_n$ vanishes for each n, i.e.

$$\int_{\mathcal{U}} 2(g-1)\frac{\partial g}{\partial \alpha_n}(-h')\,\mathrm{d}x = 0, \quad n = 1,2,3,\ldots. \tag{4.17}$$

Rearranging gives the infinite system for $\boldsymbol{\alpha} = (\alpha_1, \alpha_2, \ldots)^{\mathrm{T}}$,

$$\boldsymbol{C}\cdot\boldsymbol{\alpha} = \boldsymbol{r}. \tag{4.18}$$

where the elements of matrix $\boldsymbol{C}$ and vector $\boldsymbol{r}$ are given by

$$C_{mn} = \int_{\mathcal{U}} \phi_m\phi_n(-h')\,\mathrm{d}x, \quad (m = 1,2,\ldots; \quad n = 1,2,\ldots), \tag{4.19a}$$

$$r_m = \int_{\mathcal{U}} \phi_m(-h')\,\mathrm{d}x, \quad (m = 1,2,\ldots). \tag{4.19b}$$

The expression for off-diagonal terms of $\boldsymbol{C}$ can be simplified by multiplying (2.11) for ϕ_m by ϕ_n, subtracting ϕ_m times the equation for ϕ_n and integrating over $\mathcal{U}$ using (2.13a) at $x = W_-$. This yields

$$C_{mn} = (\lambda_m - \lambda_n)^{-1}[\phi_m'\phi_n - \phi_n'\phi_m]_{x=0} \quad (m \neq n). \tag{4.20}$$

Matrix $\boldsymbol{C}$ is symmetric. For the upward escarpments of §2 (where the downslope is absent and $W_+ = 0$) (2.13b) and (4.20) show the off-diagonal elements of $\boldsymbol{C}$ to be zero. System (4.18) then gives immediately the explicit values (2.18) for the wave amplitudes. For a ridge (where a downslope is present and $W_+ > 0$) the off-diagonal terms of $\boldsymbol{C}$ are non-zero. The orthogonality of the ϕ_n over the whole interval $W_- \leqslant x \leqslant W_+$ gives the alternative expression to (4.19a) for the coefficients,

$$C_{mn} = \int_{\mathcal{D}} h'\phi_m\phi_n\,\mathrm{d}x \quad (m \neq n). \tag{4.21}$$

The ϕ_m, ϕ_n decay exponentially and monotonically over $\mathcal{D}$ from their extrema at $x = 0$, with higher modes decaying more rapidly. The C_{mn} are thus positive and decrease rapidly in magnitude with increasing n or m for $n \neq m$. High modes are almost orthogonal on $\mathcal{U}$ and the diagonal terms of $\boldsymbol{C}$ dominate. Matrix $\boldsymbol{C}$ thus is invertible. For general ridge profiles the diagonal terms of $\boldsymbol{C}$ and the components of the vector $\boldsymbol{r}$ can only be determined numerically. Since (4.20) gives the off-diagonal elements explicitly the timing of the computation increases only linearly with the

number of modes retained even though the modes are not orthogonal over the range of interest. Once the α_n are determined from (4.18), the sum (2.16) defines $g(x)$ for all x and (4.14) gives $a(x)$. In particular

$$A = [h(0) + s^{\mathrm{T}} C^{-1} r]/h(W_+), \tag{4.22}$$

where

$$s_n = \int_{\mathscr{D}} h' \phi_n \, \mathrm{d}x \quad (n = 1, 2, \dots). \tag{4.23}$$

Expression (4.22) is independent of the normalization of the ϕ_n. For upward escarpments $\mathscr{D}$ is absent, $s = 0$, $A = 1$, and $r \neq 0$ as in §2. For downward escarpments $\mathscr{U}$ is absent, $r = 0$, and $A = h_\infty^{-1}$ as in §3.

An approximate solution to (4.18) can be found by noting that for sufficiently large n the ϕ_n are negligible in $\mathscr{D}$ and so arbitrarily extending the integrals in (4.21) to the whole interval $W_- \leqslant x \leqslant W_+$. Then once again the off-diagonal terms of C vanish and (4.18) has an explicit solution giving the ratio of amplitudes of successive modes as

$$\alpha_{n+1}/\alpha_n = \langle 1, \phi_{n+1} \rangle \, \|\phi_n\|^2 / \langle 1, \phi_{n+1} \rangle \, \|\phi_{n+1}\|^2. \tag{4.24}$$

This is precisely the ratio of the amplitudes of modes in the upper and lower bounds derived by Killworth (1989). The bounds thus correspond to the surface elevation being constant across the whole ridge but discontinuous in general at the ridge edges. The bounds are thus achieved only for upward escarpments.

A closer approximation is given by noting that since the rate of exponential decay in $\mathscr{D}$ of the ϕ_n increases with increasing n, the s_n decrease rapidly with n and the dominant contribution to A comes from the lowest modes, predominantly from the first for ridges of width unity or more. Truncating (4.18) at $n = 1$ gives the amplitude estimate

$$A h_\infty \approx h(0) + \int_{\mathscr{D}} \phi_1 h' \, \mathrm{d}x \int_{\mathscr{U}} \phi_1 h' \, \mathrm{d}x \Big/ \int_{\mathscr{U}} \phi_1^2 h' \, \mathrm{d}x, \tag{4.25}$$

where ϕ_1 is the fundamental mode. Section 6 gives comparisons of this estimate with the exact solution. Estimates of the amplitudes of the long waves follow from neglecting the off-diagonal terms of (4.18) to give

$$\alpha_n \approx \int_{\mathscr{U}} \phi_n h' \, \mathrm{d}x \Big/ \int_{\mathscr{U}} \phi_n^2 h' \, \mathrm{d}x. \tag{4.26}$$

5. Valleys

The wall-layer relations showing conservation of mass above downslopes (4.8) and constant surface elevation above upslopes (4.11) hold irrespectively of the number or order of slopes. In particular the results of the previous section extend directly to valleys. Consider a simple valley where the depth increases monotonically for a downslope region $\mathscr{D}$ ($W_- \leqslant x \leqslant 0$) and then decreases monotonically for an upslope region $\mathscr{U}$ ($0 \leqslant x \leqslant W_+$). Integrating (4.8) and (4.12) along the wall and matching at the valley edges gives the surface elevation

$$a(x) = \begin{cases} 1, & \text{in } \mathscr{I}, \\ \left(1 + \displaystyle\int_{W_-}^{x} h' g \, \mathrm{d}x\right)\!\big/ h(x), & \text{over } \mathscr{D}, \\ A, & \text{over } \mathscr{U} \text{ and } \mathscr{T}, \end{cases} \tag{5.1}$$

where the amplitude of the transmitted Kelvin wave is given by

$$A = \left(1 + \int_{\mathcal{D}} h'g\,\mathrm{d}x\right)\big/h(x). \tag{5.2}$$

The solution of system (4.18) with elements given by (4.21) gives the amplitudes in expansion (2.16) for a function equal to unity over $\mathcal{U}$. The required coefficients for g, which is identically equal to A over $\mathcal{U}$ by (4.12) and (5.1), are thus given by

$$\boldsymbol{\alpha} = A\boldsymbol{C}^{-1}\boldsymbol{r}. \tag{5.3}$$

The discussion on $\boldsymbol{C}$ and $\boldsymbol{r}$ following (4.18) carries over unchanged. Substituting (5.2) in (5.3) gives

$$A = (1 + A\boldsymbol{s}^{\mathrm{T}}\boldsymbol{C}^{-1}\boldsymbol{r}/h(0),$$

i.e.

$$A = [h(0) - \boldsymbol{s}^{\mathrm{T}}\boldsymbol{C}^{-1}\boldsymbol{r}]^{-1}. \tag{5.4}$$

Again $A = h_{\infty}^{-1}$ for downward escarpments, where $\mathcal{U}$ is absent, $\boldsymbol{s} = \boldsymbol{0}$, but $\boldsymbol{r} \neq \boldsymbol{0}$; and $A = 1$ for upward escarpments, where $\mathcal{D}$ is absent and $\boldsymbol{r} = \boldsymbol{0}$. The amplitude estimate analogous to (4.25) is

$$A^{-1} \approx h(x_0) - \int_{\mathcal{D}} \phi_1\,h'\,\mathrm{d}x \int_{\mathcal{U}} \phi_1\,h'\,\mathrm{d}x \Big/ \int_{\mathcal{U}} \phi_1^2\,h'\,\mathrm{d}x. \tag{5.5}$$

6. Specific ridges and valleys

6.1. *An exponential ridge*

As an example of a complete solution including short-wave contributions outside wall layers consider the symmetric piecewise exponential ridge of minimum depth h_1 given by

$$h = \begin{cases} 1, & |x| \geqslant W, \\ h_1\,\mathrm{e}^{\beta|x|}, & |x| \leqslant W, \end{cases} \tag{6.1}$$

with $\beta = -(1/W)\log h_1$ so $\beta > 0$ for $h_1 < 1$. As for the short-wave envelope eigensolutions of §3 there is no useful simple analytical form for the long-wave eigensolutions λ_n, ϕ_n for this profile. Further, since h' is not single-signed over the ridge (2.11) does not lead to a standard Sturm–Liouville problem. A solution follows for this simple ridge by dividing the domain into regions $-W \leqslant x < 0$ where $h' < 0$, and $0 < x \leqslant W$ where $h' > 0$, integrating inwards in each domain from the extremes $x = \pm W$ and matching at $x = 0$. Routine D02KEF again proved efficient, returning both ϕ_n and ϕ_n' and hence allowing direct evaluation of the off-diagonal terms of $\boldsymbol{C}$ through (4.20). Expression (4.18) gives the modal amplitudes α_n, (4.4) the inner limit $g(x)$ of the long-wave solutions and (4.13) the surface elevation $a(x)$ at the wall. These determine $\mathcal{L}$ and the amplitude A of the transmitted Kelvin wave in (4.15) and hence give the geostrophic component of the solution by fast Fourier inversion of the analogous integral to (2.25). This completes the determination of the long-wave and geostrophic fields. For the present exponential topography the full short-wave field for inviscid barotropic flow can also be found. Expression (3.15) for the wavefield above the downslope in the neighbourhood of the wall gives the amplitude of the short-wave field at the wall as $a(x) - g(x)$. The short-wave envelope is thus given by (3.15) with modal amplitudes

$$\alpha_n = \int_{\mathcal{D}} h'(a - g)\,\psi_n\,\mathrm{d}x \Big/ \int_{\mathcal{D}} h'\psi_n^2\,\mathrm{d}x. \tag{6.2}$$
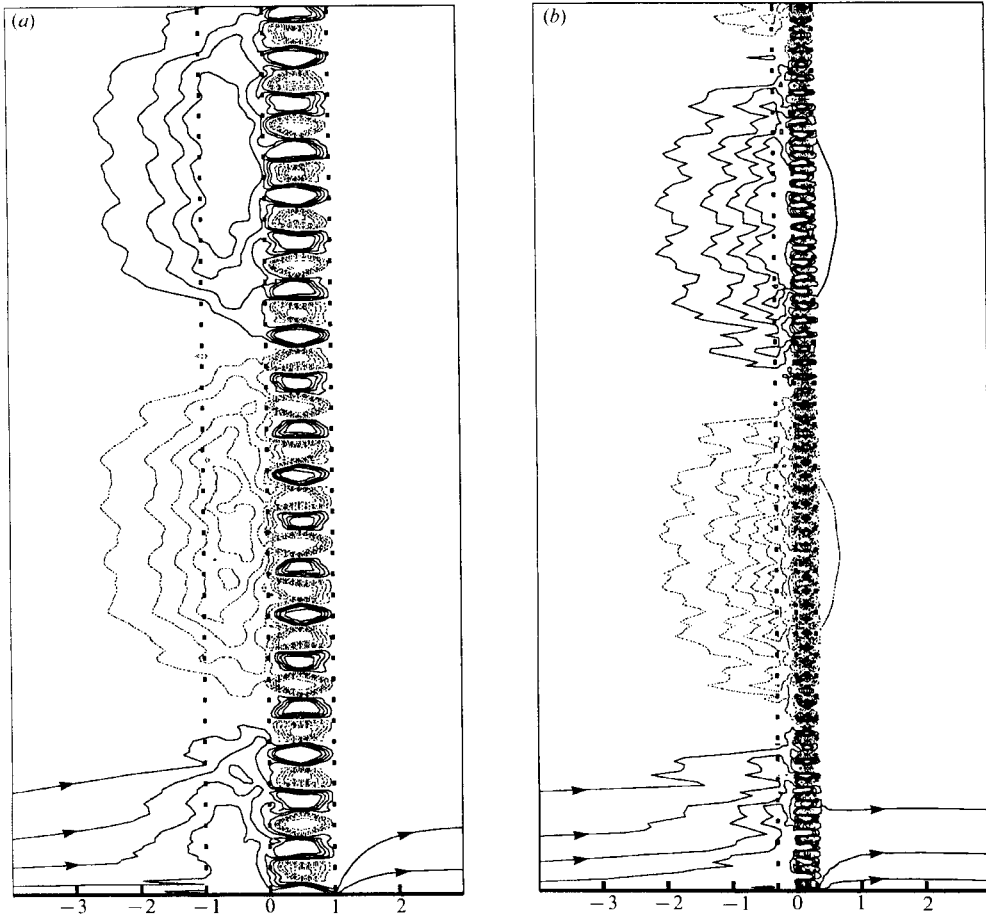
FIGURE 5. Contours of surface elevation for a Kelvin wave incident on an exponential ridge of minimum depth $h_1 = 0.5$. (*a*) $W = 1$. For a ridge of width of order the external Rossby radius or larger almost all the incident flux passes through the source at $(W, 0)$. (*b*) $W = 0.3$. For narrower ridges the long-wave field extends across the ridge providing an alternative path for some of the incident fluid. Away from the downslope region where short waves dominate the contours are streamlines for the flow.

Figure 5 gives contours of surface elevation for ridges of minimum depth $h_1 = 0.5$ and widths $W = 1$ and $W = 0.3$. The wavelengths of both the long and short waves scale on the ridge width for $W \leqslant 1$ and so are shorter above the narrower ridge. The long waves penetrate across the narrower ridge into the flat transmission region with the flux $\mathscr{L}$ differing significantly from zero.

6.2. *Triangular ridges and valleys*

As an example of a non-monotonic profile whose associated long-wave modes can be found analytically and thus be evaluated directly to arbitrary accuracy consider the symmetric piecewise linear triangular profile

$$h = \begin{cases} 1, & |x| \geqslant W, \\ h_1 + (1 - h_1)|x|/W, & |x| \leqslant W. \end{cases} \tag{6.3}$$

For $h_1 < 1$ this gives a ridge and for $h_1 > 1$ a valley. Following the analysis of §2.5
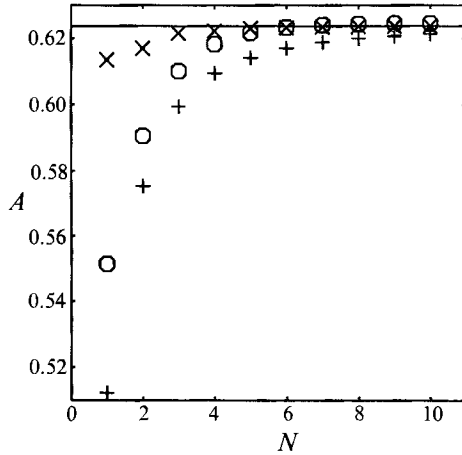
FIGURE 6. Convergence of the transmitted amplitude with increasing numbers of retained modes for a triangular ridge of half-width $W = 1$ and height $h_1 = 0.5$. The crosses give the solution obtained by truncating (4.18) and in particular approximation (4.25) is given by $N = 1$. The values obtained from an evenly spaced stepped approximation, with N steps for each slope, are given by pluses. The improved approximation using Tchebychev points to take account of high-wavenumber contributions whenever h' vanishes is given by circles.

and matching ϕ and ϕ' across $x = 0$, $\pm W$ leads to (2.30) for $-W \leqslant x \leqslant 0$ and for $0 \leqslant x \leqslant W$,

$$\phi = (K^1/I^0)I_0(\kappa X) - (I^1/I^0)K_0(\kappa X), \quad 0 \leqslant x \leqslant W, \tag{6.4}$$

where I_0, K_0, I_1, K_1 are the modified Bessel functions; Y^1, J^0, J^1, X_0, X_1 and X are given in §2.5; and

$$\left.\begin{aligned} I^1 &= 2X_1 I_0(\kappa X_1) + \kappa I_1(\kappa X_1), \\ K^1 &= 2X_1 K_0(\kappa X_1) - \kappa I_1(\kappa X_1), \\ I^0 &= K^1 I_0(\kappa X_0) - I^1 K_0(\kappa X_0), \end{aligned}\right\} \tag{6.5}$$

and $\kappa = (k^2 + X_1^2)^{\frac{1}{2}}$ where the x-wavenumber k is determined by

$$\kappa K^1 I_1(\kappa X_0) + \kappa I^1 K_1(\kappa X_0) = -kY^1 J_1(kX_0) + kJ^1 Y_1(kX_0). \tag{6.6}$$

For a ridge the associated eigenvalue is given by (2.32) and is positive. For a valley the eigenvalue is given by $-\lambda$. Solution (2.30), (6.4) yields long waves travelling outwards along a ridge and inwards above a valley. As the profile is symmetric the oppositely propagating long waves are given by reflecting these solutions about $x = 0$ and changing the sign of the eigenvalue.

   Computations for this example are particularly simple as integrals of the form (2.34) give explicit formulae for r, s and the indefinite integrals of (4.13) and (5.1). Figure 6 shows the convergence of the transmitted amplitude with increasing numbers of included modes for a triangular ridge of height $h_1 = 0.5$ and width $W = 1$. The crosses give the amplitude obtained by truncating (4.18) at $N = 1, 2, \ldots, 10$ modes. The approximation (4.25) is given by $N = 1$ and is within 1.5 % of the exact answer. The pluses give the results from the stepped-topography approximation of I, obtained by dividing the upslope and downslope into N equal intervals. This approximation is within 1 % by $N = 6$ but further improvement is slow due to Gibbs phenomena at $x = 0$, $\pm W$ (where h' vanishes). A more efficient choice of steps is to concentrate points near these singular regions. The circles in figure 6 give the transmitted amplitude obtained from I by choosing points between successive zeros
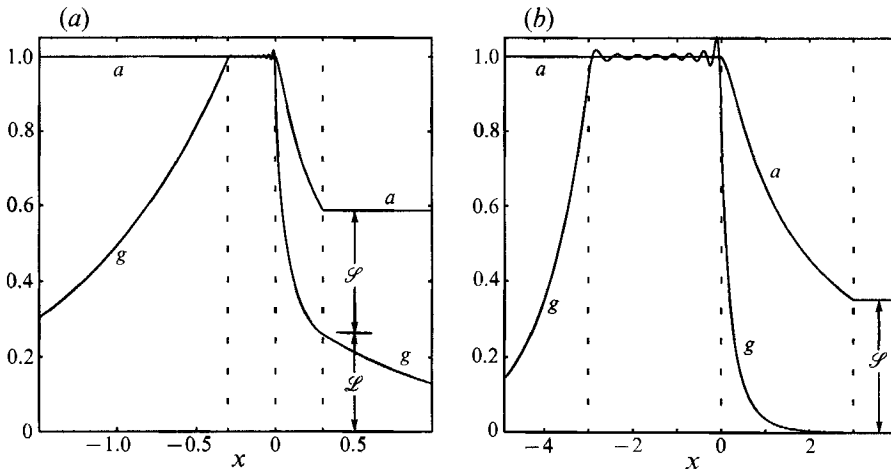
FIGURE 7. The surface elevation at the wall $a(x)$ and the inner limit of the outer-y long-wave solution $g(x)$, determined by the sum of sixteen modes on $Y = 0$, for a triangular ridge of minimum depth $h_1 = 0.3$. (*a*) A narrow ridge, $W = 0.3$. Of the transmitted flux almost half, denoted $\mathscr{L}$, is carried inwards along the far side of the ridge by the long-wave field. (*b*) A wide ridge, $W = 3$. With exponentially small error, the whole transmitted flux emerges through a source of strength $\mathscr{S}$ at $(W, 0)$.

of h' to be the Tchebychev points. For a profile where h' vanishes in $|x| > W$ and passes through zero only at $x = 0$ these are

$$x_n = \begin{cases} -\tfrac{1}{2}W\{1 + \cos\left[n\pi/(N+1)\right]\} & (-W < x < 0), \\ -\tfrac{1}{2}W\{1 - \cos\left[n\pi/(N+1)\right]\} & (0 < x < -W), \end{cases} \tag{6.7}$$

$n = 1, 2, ..., N$. By $N = 6$ this gives an error of less than 0.1%, and appears to give the most straightforward method of analysing complex topography.

Figure 7 gives the surface elevation against the wall $a(x)$ and the surface elevation $g(x)$ at the inner limit of the outer-y long-wave region $(Y \to 0)$ for a ridge of minimum depth $h_1 = 0.3$. Only sixteen terms are used in the summation to demonstrate the Gibbs phenomena, weak at $x = -W$ and stronger at $x = 0$. Figure 7(*a*) shows a narrow ridge $(W = 0.3)$ where the long-wave field still has significant amplitude at $x = W$. The surface elevation is constant along the wall until the ridge crest and then decays over the downslope $\mathscr{D}$. The inner long-wave elevation $g(x)$ equals $a(x)$ over the upslope $\mathscr{U}$, decaying exponentially on both sides of $\mathscr{U}$. Of the transmitted mass flux $A = a(W)$, almost half $(\mathscr{L} = g(W))$ is carried by the long-wave field along the far side of the ridge with the remainder emerging from a source at $(0, W)$ of strength $\mathscr{S} = a(W) - g(W) = A - \mathscr{L}$. Figure 7(*b*) shows a wide ridge $(W = 3)$ where the long waves have negligible amplitude at $x = W$ and so the whole transmitted flux A emerges through a source of strength $\mathscr{S} \approx A$. The figure shows how the geostrophic region elevation in $\mathscr{D}$ decreases towards its wide-topography limit of $g \equiv 0$ as W increases. Figure 8 gives flow patterns for ridges of minimum depths $h_1 = 0.5$. For the narrow ridge $(W = 0.3)$ of figure 8(*a*) the fraction $\mathscr{L}$ of the incident flux passes directly across the ridge. Figure 8(*b*) is shown with a width of $W = 1$ rather than $W = 3$ as already to within the accuracy of the plotting all fluid enters the wall layer above the downslope and leaves through a source at $(W, 0)$. The stippling along the wall $y = 0$ in $x > W$ shows the region of thickness B occupied by internal Kelvin waves when $\omega \ll B \ll 1$. In this limit the external Kelvin wave carries all the
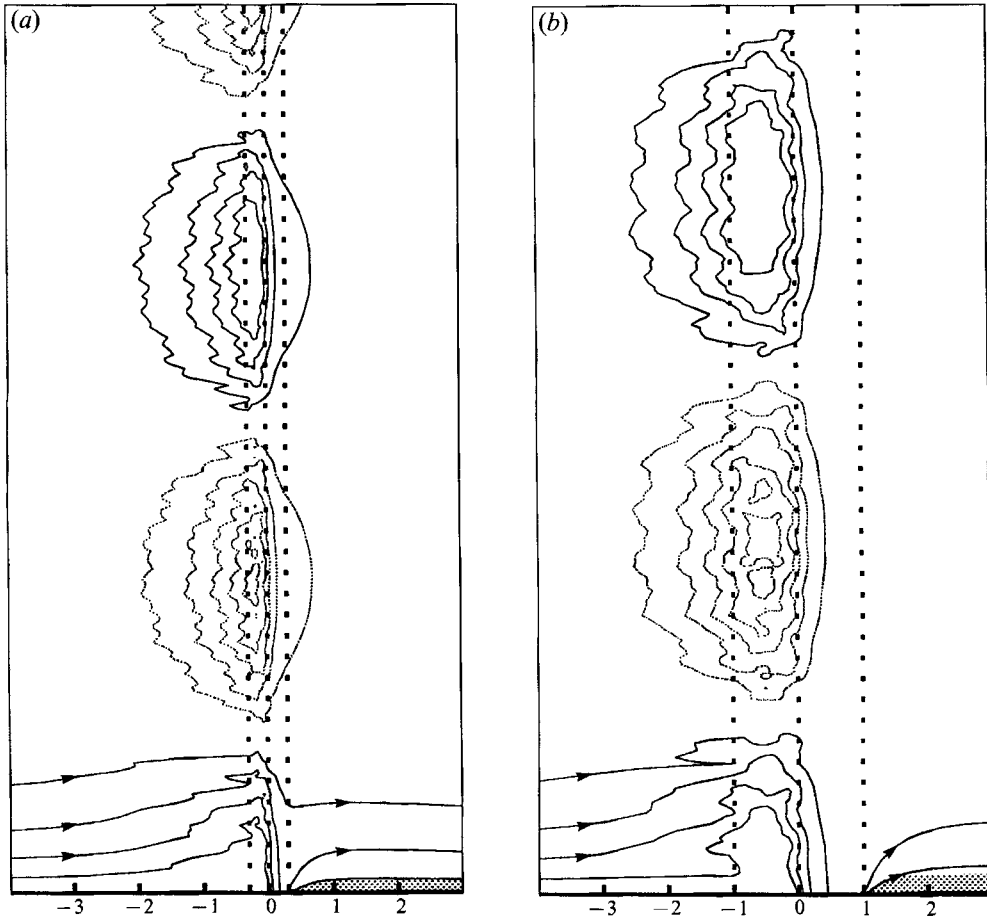
FIGURE 8. Contours of surface elevation for a Kelvin wave incident on a triangular ridge of minimum depth $h_1 = 0.5$. (a) A narrow ridge, $W = 0.3$. A fraction $\mathscr{L}$ of the incident flux passes directly over the ridge. (b) A wide ridge, $W = 1$. Almost the entire flux enters the wall-layer above the downslope and is expelled through the source at $(W, 0)$. The stippling along the wall $y = 0$ in $x > W$ shows the region of thickness B occupied by internal Kelvin waves when $\omega \ll B \ll 1$.

transmitted mass flux and the higher-order internal Kelvin waves carry the remainder of the transmitted energy flux.

Figure 9 gives a and g for a valley of maximum depth $h_1 = 3$. The Gibbs phenomena are now at the slope breaks at $x = 0$ and $x = W$. The surface elevation at the wall decays from its unit incident value over the downslope $\mathscr{D}$, and then remains constant at its transmitted value A after the valley bottom. The geostrophic elevation g is raised to A over the upslope $\mathscr{U}$, again decaying exponentially on both sides of $\mathscr{U}$. Figure 9(a) gives a and g for a narrow valley ($W = 0.3$) showing that about a third of the incident flux ($\mathscr{L} = g(-W)$) is turned outwards as a Kelvin wave running along $x = -W$ before the valley and about two-thirds ($\mathscr{S} = a(-W) - g(-W)$) enters the boundary layer through a sink at $(-W, 0)$. Since $a(W) = g(W)$ there is no source on the far side of the valley. Figure 9(b) gives a and g for a wide valley ($W = 3$), showing that almost the entire incident flux enters the boundary layer. Once again g decreases over $\mathscr{D}$ with increasing W although, as noted in I, the approach to its wide-topography limit of $g \equiv 0$ is slower than in figure 7 as the Rossby radius is larger above the valley.
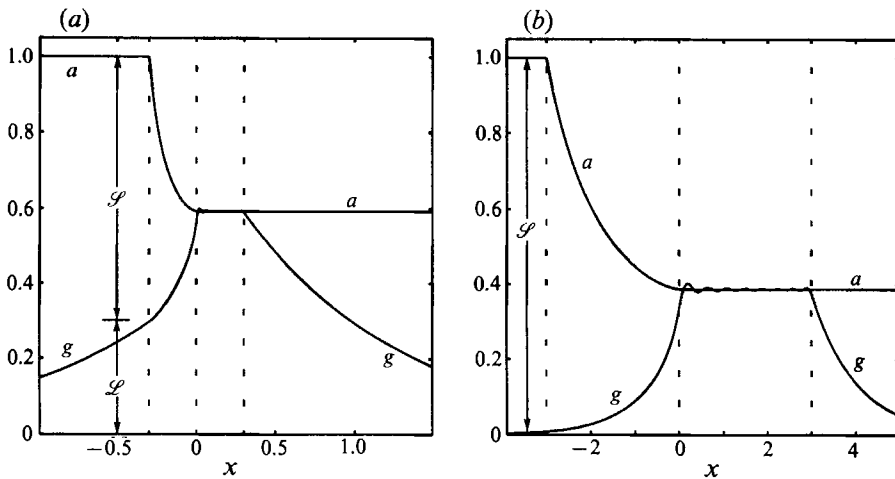
FIGURE 9. The surface elevations a and g for a triangular valley of maximum depth $h_1 = 3$. (a) A narrow valley, $W = 0.3$. Of the incident flux about one third, denoted $\mathscr{S}$, is carried outwards along the near side of the valley by the long-wave field and the remaining two-thirds enters the wall layer. (b) A wide valley, $W = 3$. Almost all the incident flux enters the wall layer through a sink of strength $\mathscr{S}$ at $(-W, 0)$.
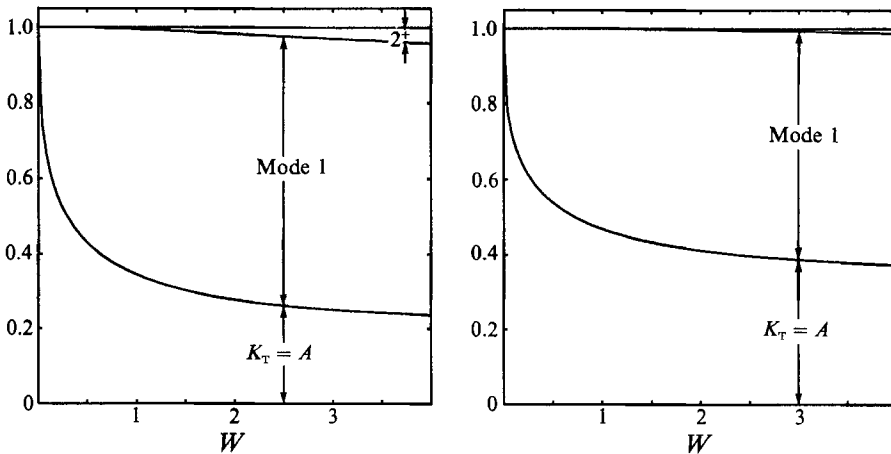

FIGURE 10. The distribution of mass flux amongst the transmitted Kelvin wave and scattered topographic long waves as a function of the half-width W, normalized on the incident flux. (a) For a ridge with minimum depth $h_1 = 0.2$ the transmitted mass flux $K_T = A$ approaches $h_1 = 0.2$ as W increases. (b) For a valley of maximum depth $h_1 = 3$ the transmitted flux approaches $A = 1/h_1 = \frac{1}{3}$ with increasing W. In both cases mass is conserved and at each W the total flux scattered into long waves is $1 - A$, carried predominantly by the fundamental mode.

Figure 10 gives the distribution of the mass flux among the wave modes as a function of feature width. For both the ridge with minimum depth $h_1 = 0.2$ of figure 10(a) and the valley with $h_1 = 3$ of figure 10(b), the fundamental long wave dominates the mass transport with negligible transport in higher modes for any width W. Since the depths in the incident and transmission regions are the same the fundamental mode here, unlike that in §2, is not anomalous for small W. As $W \to 0$ its wavelength and amplitude in the scattered field, like those of the higher modes, vanishes. This contrasts with the behaviour as $W \to 0$ for topographies like the escarpment of figure 3 across which there is a net change of depth. For all widths W
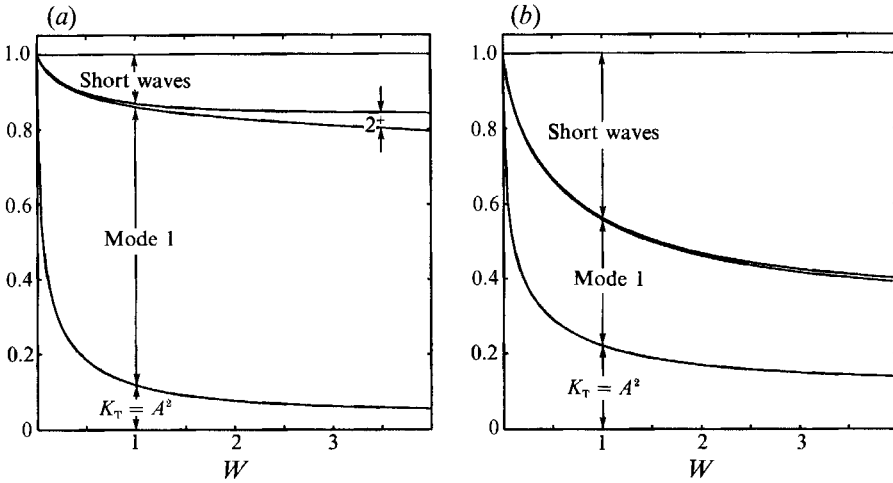
FIGURE 11. The distribution of energy flux amongst the transmitted Kelvin wave, the scattered topographic long waves and scattered short waves, normalized on the incident flux, as a function of the half-width W for the same features as figure 5. (a) For the ridge the transmitted flux $K_T = A^2$ approaches $h_1^2 = 0.04$, the flux scattered into long waves approaches $1 - A = 0.8$, and the flux scattered into short waves approaches $A(1-A) = 0.16$. (b) For the valley the corresponding limiting values are: transmitted flux, $A^2 = 1/h_1^2 = \frac{1}{9}$; long waves, $A(1-A) = \frac{2}{9}$; and short-waves $1 - A = \frac{2}{3}$.

the total mass flux is unity as expected, with the transmitted Kelvin wave carrying flux A and the scattered long waves varying flux $1 - A$. That this holds for any ridge or valley follows by direct integration of the long-wave flux, $\int_{-\infty}^{\infty} g' h \, dx$, using (4.13) and (5.1). Figure 11 gives the distribution of energy flux among the wave modes for the same profiles as figure 10. Once again the dominant long-wave mode is the fundamental and high modes carry little energy. A significant fraction of the incident energy is however dissipated in the wall layer or scattered outwards as short waves. Consider a wide ridge of minimum depth h_1. Before the ridge the amplitude a, mass and energy fluxes and depth are unity. After the upslope the depth is h_1, the amplitude remains unity and so the mass and energy fluxes are h_1. The energy and mass transported outwards by long waves are thus both $1 - h_1 = 1 - A$ as in §2. After the downslope the depth is again unity, the amplitude $A = h_1$ and the transmitted mass and energy fluxes are A and A^2 respectively. Hence the short waves over the downslope carry no mass but have outwards energy flux $A(1-A)$ with maximum value $\frac{1}{4}$ for a ridge of half the fluid depth. By $W = 4$ in figure 11(a) these asymptotic values have been closely achieved. For a wide valley of maximum depth h_1 the mass flux over the valley floor is unity so the amplitude and energy flux are both $1/h_1$. The short waves over the downslope carry no mass but have outward energy flux $1 - 1/h_1 = 1 - A$ as in §3. After the upslope the amplitude remains $A = 1/h_1$ and the transmitted mass and energy fluxes are A and A^2. Hence the long waves carry outward a mass flux of $1 - A$ which has a maximum value of $\frac{1}{4}$ for a valley of depth twice the far-field depth. Over a valley it is the long-wave field whose energy is bounded above to be less than one quarter the incident energy, whereas over a ridge it is the short-wave field that is so bounded. Although approaching their asymptotic values, the fluxes in figure 11(b) do not approach as closely as those in figure 11(a) until W is of order 10 owing to the larger Rossby radius above the valley. Unlike the simple expressions for the partitioning of the mass flux, those for the energy flux hold only in the wide-feature limit.
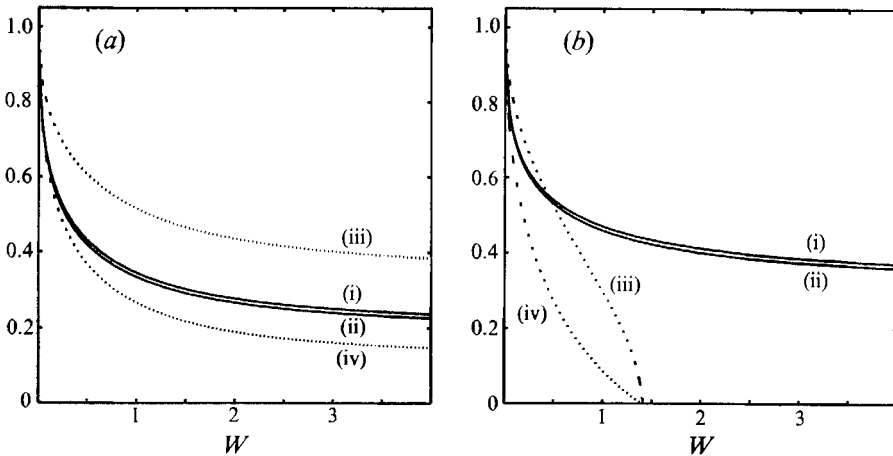
FIGURE 12. Bounds and approximations to the transmitted amplitude as a function of the half-width W: (i) the exact value; (ii) the one-mode approximation (4.25); (iii), (iv) the upper and lower bounds from Killworth (1989). (a) A ridge of minimum depth 0.2. (b) A valley of maximum depth 3.

Figure 12 gives the one-mode approximation (4.25) and the upper and lower bounds of Killworth (1989). As the bounds are derived neglecting energy in the short-wave field they are achieved only above upward escarpments.

7. Discussion

An explicit solution method has been derived for the scattering of Kelvin waves by continuous topography and the structure of the solution at low frequencies obtained. The wavefield is most straightforward over upward escarpments where only long waves are present and the surface elevation at the wall is constant. Over downward escarpments the scattered topographic field contains only short waves. For exponential topography a complete description of the flow field follows by separating the rapidly varying phase and slowly moving group velocity components but for general topography where ray paths are not straight no simple closed-form description of the complete short-wave field is possible. However, analysis of the short waves within a distance ω of the wall $y = 0$ where they are generated leads to a differential equation for mass conservation that relates the inner limit of the outer long-wave flow to the surface elevation at the wall. Together with a radiation condition this allows a complete solution for the barotropic long-wave field and in particular determines the amplitude of the transmitted Kelvin wave. An explicit form for the whole short-wave field is not required.

Vanishingly small dissipation and weak stratification ($\omega \ll B \ll 1$) both cause short waves to decay exponentially with distance from the wall $y = 0$. Outside these wall layers the long-wave and geostrophic fields derived here give the complete flow pattern in these limits. The short waves carry no mass. In the weakly dissipative limit their energy is destroyed within a thin wall layer above downslopes. In weakly stratified flow this energy is scattered into internal Kelvin waves which are transmitted past the topography propagating along the wall $y = 0$ confined within a layer of dimensional thickness $N_0 H/f$. With stratification increasing from barotropic flow where $B \ll \omega \ll 1$ to weakly stratified flow with $\omega \ll B \ll 1$ the long-waves fields are unaltered but the short-wave energy changes smoothly from being

scattered outwards along downslopes to being transmitted along the wall. The transmitted energy flux increases with the ratio B/ω but the transmitted mass flux remains constant.

The present method confirms the accuracy of the apparently crude stepped-topography approximation for similar problems presented in I, placing the analysis there into the more usual context of solution by mode matching and elucidating some of the structures that appear in the discrete problem as the resolution is increased. For general continuous topography the eigenfunctions for the long-wave modes can be found only numerically and hence the choice in solution is between solving the exact problem approximately, truncating at a fixed number of modes as discussed here, or solving an approximating problem exactly as in I. If the topography is complicated or the transmission amplitude alone is required then the stepped-topography approximation of I appears greatly superior. If the topography is simple and the fundamental topographic mode easy to obtain then the present analysis yields a simple but accurate approximation directly. The details derived here for the structure of the continuous problem enable the efficiency of the previous stepped-topography approximation to be greatly improved. The stepped approximation is optimized by dividing the domain into intervals bounded by those places where h' vanishes and concentrating the approximating points near the ends of the intervals.

The solutions here give the surface elevation to zero order in the frequency $\omega \ll 1$. Although the surface elevation is continuous everywhere the velocity parallel to the topography, $v = \eta_x$, is discontinuous at the edges of the topography and whenever h' vanishes (e.g. ridge crests and valley floors). This discontinuity forces the leading-order correction to the flow field. For the upslope of §2, η_x is discontinuous at $x = W_-$ and $x = 0$ for y of order unity. This discontinuity forces waves varying rapidly in x with scale $\omega^{\frac{1}{2}} \ll 1$. Over $\mathscr{U}$ the solution contains an extra term of form

$$\omega^{\frac{1}{2}} \eta^h(\xi, x, y), \tag{7.1}$$

where $\xi = x/\omega^{\frac{1}{2}}$. Noting that the leading-order solution is constant over $\mathscr{U}$ and substituting in (2.1) gives the leading-order problem in a WKB expansion for η^h

$$i\eta^h_{\xi\xi} + (h'/h)\,\eta^h_y = 0 \quad \text{over } \mathscr{U}, \tag{7.2}$$

$$\eta^h_x = \partial_x \eta_i(W_-, y) \quad (x = W_-), \qquad \eta^h_x = \partial_x \eta_i(0, y) \quad (x = 0), \tag{7.3}$$

$$\eta^h = 0, \quad y = 0, \quad \text{over } \mathscr{U}. \tag{7.4}$$

Equation (7.2) is a form of the long-wave equation since the x-scale of the motion is much smaller than the y-scale and h'/h gives the slowly varying (in ξ) local slope. A complete solution to the problem posed by (7.2)–(7.4) can be derived by Fourier integral techniques. To determine the general form of the extra term η^h it is sufficient to note that solutions of (7.2) represent a high-x-wavenumber field forced at the escarpment edges and spreading rapidly on the inner-y scale to cover the whole upslope in inviscid flow or remaining confined to the escarpment edges as in Johnson (1989a) in weakly dissipative flow. This term gives the leading-order correction to the flow field representing an additional mass flux of order $\omega^{\frac{1}{2}}$ and energy flux of order ω.

A similar high-x-wavenumber contribution is forced by the discontinuity in the leading-order η_x at a ridge crest or valley floor. Consider a profile that is locally parabolic at $x = 0$ so $h'(0) = 0$ but $h''(0) \neq 0$. Then the relevant short scale is $\xi_1 = x/\omega^{\frac{1}{3}}$ and (2.1) gives to leading order

$$i\eta^h_{\xi_1\xi_1} - \xi_1(h''/h)\,\eta^h_y = 0, \tag{7.5}$$

where here the extra term over the topography is of the form $\omega^{\frac{1}{3}} \eta^h(x/\omega^{\frac{1}{3}}, x, y)$. Solutions of (7.5) behave as Airy functions in ξ_1, being oscillatory on upslopes (where $h''(0) \operatorname{sgn} x$ is negative for both ridges and valleys) and decaying exponentially over downslopes (where $h''(0) \operatorname{sgn} x$ is positive). This term is larger than the correction at escarpment edges although the correction there would also be of order $\omega^{\frac{1}{3}}$ if the slope were continuous but h'' discontinuous, i.e. the escarpment edges were locally parabolic.

The results of §§2–4 were presented for profiles without plateaux, i.e. finite intervals of x where h' vanishes. The long-wave modes ϕ_n no longer form a complete set above profiles with plateaux and an arbitrary function of x cannot be expanded there in terms of the ϕ_n alone. The outer limit of the inner solution is not however completely arbitrary. Above flat regions the inner region satisfies (2.4b) and as $y \to \infty$ the y-dependence decays exponentially to leave the outer limit of the inner solution satisfying

$$h\eta_{xx} - \eta = 0 \quad (y \to \infty, \quad h' = 0). \tag{7.6}$$

This is precisely the form of (2.11) above plateaux, satisfied by each long-wave mode. Expression (2.16) for the inner limit of the outer-y solution is thus sufficient to match the outer limit of any possible inner solution. The present results thus apply equally to profiles with plateaux and the matching above plateaux is automatic. Integrals like (2.18) thus do not depend explicitly on values where $h' = 0$. The precise form of the flow above plateaux can be found as in I where the topography consists solely of vertical escarpments separated by plateaux. In general the flow above plateaux in upslopes is stagnant with the surface elevation taking the same constant value as over the remainder of the upslope. Over downslopes the fluid carried by the wall layer escapes through a source on the wall at the leading edge of the plateau and spreads over the plateau before contracting to pass into a sink on the wall at the trailing edge of the plateau and entering a new wall-layer. Such flows are illustrated in I.

The comments in I on non-rectilinear topography apply here also. In the geostrophic region (2.4a) implies that the surface elevation is constant along isobaths. Thus for a given far-field profile the solution is unaltered if the bounding wall is not planar or if the isobaths are not straight, provided solely that all far-field isobaths reach the wall. If a ridge is broken by a gully or a valley by a bridge then some far-field isobaths do not reach the wall. Values of $g(x)$ above the isobaths that curve back are then related by connection formulae as in Johnson (1989b) and the transmitted Kelvin wave is stronger as in I.

The profiles considered in §6 are symmetric. An example of an asymmetric profile is considered in I, where it is noted that reflecting a ridge or valley profile leaves the transmitted Kelvin wave amplitude unaltered when the far-field depths on each side of the profile are equal. This is a special case of the result proved in Appendix A that *the transmitted mass flux is invariant under reflection at arbitrary subinertial frequencies.* From the example in I it appears that maximum blocking occurs for the Steiner symmetrization of a given ridge or valley profile.

Appendix A. The adjoint problem

The adjoint problem follows most straightforwardly by reversing the direction of the rotation. The incident Kelvin wave then travels inwards from $x = \infty$ and is scattered into outwardly propagating topographic waves by the ridge. A transmitted wave continues onwards to $x = -\infty$. Let η and U give the spatial dependence of the

surface elevation and velocity fields in the original problem and let the corresponding surface elevation and velocity fields for the adjoint problem be q and V. Then q satisfies, from (2.8) in I,

$$-\mathrm{i}\omega(1-\omega^2)\,q = \nabla\cdot(hV). \tag{A 1}$$

Taking $\eta\times(A\,1)+q\times(2.8)$ of I gives

$$\nabla\cdot(H\eta V+HqU) = 0. \tag{A 2}$$

Integrating (A 2) over a sufficiently large rectangle $0\leqslant y\leqslant y_1$, $-x_1\leqslant x\leqslant x_1$ and noting that for the Kelvin waves,

$$U\cdot i = -(1-\omega^2)\,\eta_y,$$

gives

$$(1-\omega^2)\,(H_\infty A - H_0 A') = \int_{-\infty}^{\infty} (H\eta V\cdot j + HqU\cdot j)\,\mathrm{d}x, \tag{A 3}$$

where A, A' are the amplitudes of the transmitted waves in the original and adjoint problems for unit-amplitude incident waves. Since the left-hand side of (A 3) is constant, the right-hand side is independent of y_1, for sufficiently large y_1. Far from the wall the topographic wave fields η and q each consist of a sum of propagating modes. Consider a typical term from each sum proportional to (say) $\exp(\mathrm{i}\lambda_1 y)$ and $\exp(\mathrm{i}\lambda_2 y)$. Then their joint contribution to the integral is proportional to $\exp[\mathrm{i}(\lambda_1-\lambda_2)\,y_1]$. Since the right-hand side is independent of y_1, this term has coefficient zero if $\lambda_1\neq\lambda_2$, i.e. for waves modes of differing wavenumber

$$\int_{-\infty}^{\infty} (H\eta V\cdot j + HqU\cdot j)\,\mathrm{d}x = 0 \quad (\lambda_1\neq\lambda_2). \tag{A 4}$$

All waves in the summation for η carry energy outwards for positive rotation whereas those in the summation for q carry energy outwards for negative rotation. Hence at fixed frequency the group velocities of the two sets of waves are in the opposite direction and so the same wavenumber cannot appear in both sums. By (A 4) the right-hand side of (A 3) vanishes giving

$$H_\infty A = H_0 A'. \tag{A 5}$$

The transmitted volume flux of the adjoint and original problems is the same. The result is valid for all subinertial ($\omega < 1$) incident waves.

Note that because of the asymmetry of the radiation conditions q cannot be identified with $\bar{p}$, the complex conjugate of p, even though they satisfy the same equation (A 1). This is a significant difference between rotating and non-rotating scattering and arises from the unidirectional propagation of waves of given shape.

Appendix B. General topography

For general topography consisting of many ridges, valleys and plateaux and possibly extending to infinity it is convenient to follow I and introduce the cumulative depth given here in terms of infinitesimals by

$$\mathrm{d}s = \begin{cases} 0 & \text{over upslopes,} \quad h'\leqslant 0, \\ \mathrm{d}h & \text{over downslopes,} \quad h'\geqslant 0, \end{cases} \tag{B 1}$$

with $s(-\infty) = h(-\infty) = 1$. Then s is a monotonically increasing function of x and for continuous h there corresponds to each x a unique s. Moreover, since a is constant

when $ds = 0$ by (4.11) and $ds > 0$ elsewhere, a is uniquely determined as a function of s and hence as a function of x. In terms of s (4.8) becomes

$$g(s) = (d/ds)\,(as).\qquad\qquad(\text{B 2})$$

Note that this form incorporates any plateaux in h automatically: the transformation to the new ordinate removes the necessity to discuss flat-topped topography separately. At plateaux in upslopes or downslopes g is continuous but dg/ds is in general discontinuous. At a ridge-crest or valley-floor plateaux g is discontinuous as a function of s.

It remains to match the outer solution (2.16) at $Y = 0$ with (B 2). The most straightforward matching follows as in I by solving (B 2) subject to the constraints (4.6) and, once a and g are determined, obtaining the coefficients α_j in (4.13) from (4.5). The simplest parameterization of (B 2) corresponds to taking $a(s)$ to have values $a_0, a_1, \ldots, a_n$ for n-values of s from $s_0 = 1$ to $s_n = s_{\max}$ where $s_{\max}$ is the maximum value of s (occurring at $x = \infty$), and forming the finite-difference approximation

$$g_j = (a_j s_j - a_{j-1} s_{j-1})/(s_j - s_{j-1}),\quad j = 1, \ldots, n,\qquad\qquad(\text{B 3})$$

as in (3.7) of I. The stepped-topography approximation of I corresponds to the simplest discretization of the continuous problem.

A more efficient discretization can be obtained by expanding $a(s)$ as a Tchebychev series with undetermined coefficients and determining the coefficients from the constraints (4.6). As $a(s)$ is continuous for all profiles and differentiable for profiles without ridge-crest or valley-floor plateaux the convergence of such expansions is guaranteed.

REFERENCES

GILL, A. E., DAVEY, M. K., JOHNSON, E. R. & LINDEN, P. F. 1986 Rossby adjustment over a step. *J. Mar. Res.* **44**, 713–738.

INCE, E. L. 1927 *Ordinary Differential Equations.* Longmans, Green and Co.

JOHNSON, E. R. 1985 Topographic waves and the evolution of coastal currents. *J. Fluid Mech.* **160**, 499–509.

JOHNSON, E. R. 1989a Boundary currents, free currents and dissipation regions in the low-frequency scattering of shelf waves. *J. Phys. Oceanogr.* **19**, 1293–1302.

JOHNSON, E. R. 1989b Connection formulae and classification of scattering regions for low-frequency shelf-waves. *J. Phys. Oceanogr.* **19**, 1303–1312.

JOHNSON, E. R. 1989c The scattering of shelf waves by islands. *J. Phys. Oceanogr.* **19**, 1313–1318.

JOHNSON, E. R 1989d Topographic waves in open domains. Part. 1. Boundary conditions and frequency estimates. *J. Fluid Mech.* **200**, 69–76.

JOHNSON, E. R. 1990 The low-frequency scattering of Kelvin waves by stepped topography. *J. Fluid Mech.* **215**, 23–44 (referred to herein as I).

JOHNSON, E. R. 1991a Low-frequency barotropic scattering on a shelf bordering an ocean. *J. Phys. Oceanogr.* **21**, 721–727.

JOHNSON, E. R. 1991b The scattering at low frequencies of coastally trapped waves. *J. Phys. Oceanogr.* **21**, 913–932.

JOHNSON, E. R. & DAVEY, M. K. 1990 Free surface adjustment and topographic waves in coastal currents. *J. Fluid Mech.* **219**, 273–289.

KILLWORTH, P. D. 1989 How much of a baroclinic coastal Kelvin wave gets over a ridge? *J. Phys. Oceanogr.* **19**, 321–341.

LONGUET-HIGGINS, M. S. 1968 Double Kelvin waves with continuous depth profiles. *J. Fluid Mech.* **34**, 49–80.

SMITH, R. 1972 The ray paths of topographic Rossby waves. *Deep-Sea Res.* **18**, 477–483.